Analytical Biochemistry **268,** 229–237 (1999)
Article ID abio.1998.3069, available online at http://www.idealibrary.com on IDEAL®

Mass Spectrometric Analysis of Catechol–Histidine Adducts from Insect Cuticle

James L. Kerwin,* Frantisek Turecek,† Rongda Xu,‡,[1] Karl J. Kramer,§ Theodore L. Hopkins,‡ Christine L. Gatlin,¶ and John R. Yates III¶

**Botany Department, Box 351330, University of Washington, Seattle, Washington 98195; †Chemistry Department, Box 351700, University of Washington, Seattle, Washington 98195; ‡Department of Entomology, Kansas State University, Manhattan, Kansas 66506; §Grain Marketing and Production Research Laboratory, ARS-USDA, 1515 College Avenue, Manhattan, Kansas 66502-2736; and ¶Department of Molecular Biotechnology, Box 357730, University of Washington, Seattle, Washington 98195-7730*

Received August 24, 1998

Adducts of catechols and histidine, which are produced by reactions of 1,2-quinones and *p*-quinone methides with histidyl residues in proteins incorporated into the insect exoskeleton, were characterized using electrospray ionization mass spectrometry (ESMS), tandem electrospray mass spectrometry (ESMS–MS, collision-induced dissociation), and ion trap mass spectrometry (ITMS). Compounds examined included adducts obtained from acid hydrolysates of *Manduca sexta* (tobacco hornworm) pupal cuticle exuviae and products obtained from model reactions under defined conditions. The ESMS and ITMS spectra of 6-(*N*-3′)-histidyldopamine [6-(*N*-3′)-His-DA, π isomer] isolated from *M. sexta* cuticle were dominated by a $[M + H]^+$ ion at *m/z* 308, rather than the expected *m/z* 307. High-resolution fast atom bombardment MS yielded an empirical formula of $C_{14}H_{18}N_3O_5$, which was consistent with this compound being 6-(*N*-1′)-histidyl-2-(3,4-dihydroxyphenyl)ethanol [6-(*N*-1′)-His–DOPET] instead of a DA adduct. Similar results were obtained when histidyl–catechol compounds linked at C-7 of the catechol were examined; the (N-1′) isomer was confirmed as a DA adduct, and the (N-3′) isomer identified as an (*N*-1′)-DOPET derivative. Direct MS analysis of unfractionated cuticle hydrolysate revealed intense parent and product ions characteristic of 6- and 7-linked adducts of histidine and DOPET. Mass spectrometric analysis of model adducts synthesized by electrochemical oxidative coupling of *N*-acetyldopamine (NADA) quinone and *N*-acetylhistidine (NAcH) identified the point of attachment in the two isomers. A prominent product ion corresponding to loss of CO_2 from $[M + H]^+$ of 2-NAcH–NADA confirmed this as being the (N-3′) isomer. Loss of (H_2O + CO) from 6-NAcH–NADA suggested that this adduct was the (N-1′) isomer. The results support the hypothesis that insect cuticle sclerotization involves the formation of C–N cross-links between histidine residues in cuticular proteins, and both ring and side-chain carbons of three catechols: NADA, *N*-β-alanyldopamine, and DOPET.

Key Words: **catecholamine; catechol; *o*-quinone; histidine; histidyl conjugate; 3,4-dihydroxyphenylethanol; oxidation; nucleophilic addition; *N*-acetyldopamine; dopamine; mass spectrometry; insect cuticle; *Manduca sexta;* tobacco hornworm.**

Posttranslational modification of peptides and proteins occurs in all eukaryotic systems (1, 2), and the roles of moieties covalently attached to these molecules including phosphate (3–5), isoprenoids and fatty acids (6, 7), and monomeric and polymeric sugars (8, 9) in regulating biological and biochemical activities have been investigated. Mass spectrometric techniques such as electrospray (ESMS),[2] ion trap (ITMS), and matrix-assisted laser desorption–time-of-flight (MALDI–TOF) are becoming routine in analyzing these modifications, although detailed structural characterization remains difficult when dealing with unknown complex samples.

[1] Current address: CombiChem, Inc., 9050 Camino Santa Fe, San Diego, CA 92121.

[2] Abbreviations used: ESMS, electrospray mass spectrometry; ITMS, ion trap MS; MALDI–TOF, matrix-assisted laser desorption–time-of-flight; DOPET, 3,4-dihydroxyphenylethanol; HMQC, heteronuclear multiple quantum coherence correlation; TOCSY, total correlation spectrometry; CID, collision-induced dissociation; RCE, relative collision energy; FAB, fast atom bombardment; DMSO, dimethyl sulfoxide; 6-(*N*-1′)-His-DA, 6-(*N*-1′)-histidyldopamine; NADA, *N*-acetyldopamine; NAcH, *N*-acetylhistidine.

0003-2697/99 $30.00

A more difficult analytical problem is encountered when dealing with biological polymers consisting of three or more different compound classes cross-linked to form complex, relatively insoluble molecules. One example of this is the exoskeleton (cuticle) of insects, which consists in part of a structurally ill-defined polymeric matrix of diphenols that are bonded to other phenols, proteins, and polysaccharides (10–12). Structural elucidation of these polymers is difficult, even when using model systems employing defined monomers reacted under controlled conditions (13–15). Classical chemical methods such as HPLC coupled with electrochemical or UV detection, and spectroscopic methods including solid-state ^{13}C and ^{15}N nuclear magnetic resonance (16–19), have yielded detailed structural information. These techniques, however, require milligram quantities of material, are not suitable for analyzing mixtures of natural products, and are unable to specify the sites of attachment between some components, e.g., a bond between a catecholic compound and histidine.

A recent study showed that ESMS and ITMS can be used to distinguish (N-1′) [denoted as N-τ] and (N-3′) [denoted as N-π] methyl-substituted histidines (20). This study presents new data obtained by ESMS–MS and ITMS–MS, which confirms the structures of four previously characterized catechol adducts from pupal cuticle exuviae of the tobacco hornworm, *Manduca sexta* (21, 22), and corrects the structures of the other two, which are adducts of 3,4-dihydroxyphenylethanol (DOPET) instead of DA.

MATERIALS AND METHODS

Isolation of cuticle adducts. Washed and air-dried pupal exuviae of *M. sexta* were ground in dry ice and lyophilized. The powder (0.25 g) was heated for 24 h at 110°C in 5 mL of 6 M HCl containing 5% phenol *in vacuo* in a 20-mL hydrolysis tube (22). Catechols were removed selectively from the hydrolysates by alumina adsorption using modifications of protocols described by Hopkins *et al.* (23).

HPLC. A binary mobile phase was used (22): solvent A—0.15 M formic acid and 0.03 M ammonium formate (pH 3.0); solvent B—MeOH and aqueous 0.3 M formic acid + 0.06 M ammonium formate (1/1, v/v). Spherisorb 5 ODS-2 (250 × 21.2 mm) and Prodigy ODS-2-PREP (10 μm, 250 × 10 mm) columns were used (Phenomenex, Torrance, CA). Catechols and their adducts were separated using the Spherisorb column, which resolved two compounds and a third fraction with two major and several minor components. The latter fraction was lyophilized, and components were separated using the Prodigy column. Four components were identified as previously described (22).

Model reactions. Large-scale synthesis of adducts of NADA quinones with *N*-acetylhistidine (NAcH) used a flowthrough coulometric cell (24). Reaction products were characterized as 6-[*N*-(*N*-acetylhistidyl)]-*N*-acetyldopamine and 2-[*N*-(*N*-acetylhistidyl)]-*N*-acetyldopamine by MALDI–TOF MS, 1D ^{1}H and ^{13}C NMR, 2D ^{13}C–^{1}H heteronuclear multiple quantum coherence correlation (HMQC), and ^{1}H–^{1}H total correlation spectroscopy (TOCSY) NMR (12). 6-*N*-Histidyl–DOPET was synthesized and purified by the method of Xu *et al.* (21), except that DOPET was used instead of NADA in the reaction mixture.

Mass spectrometry. The ESMS and ESMS–MS spectra were obtained using a tandem quadrupole Sciex API III instrument (PE/SCIEX Thornhill, Ontario, Canada). Samples were infused into the electrospray source via a 50-μm i.d. fused silica transfer line using a Harvard Apparatus pump at 0.4–2 μL/min. The interface was modified as described by Wang *et al.* (25), which allowed acquisition of high-quality spectra at reduced flow rates. Approximately 10–50 pmol of sample were used to obtain individual spectra. Positive ion ESMS and ESMS–MS spectra were acquired using orifice voltages from 25 to 110 V. The interface temperature was maintained at 52°C. For tandem mass spectrometry (MS–MS), precursor ions were selected with the first quadrupole (Q1) for collision-induced dissociation (CID) with argon in the second quadrupole (Q2). The third quadrupole (Q3) was scanned with a mass step of 0.10–0.20 μ and 1 ms/step. Parameters were sufficient to usually obtain a valley of 1 to 18% between peaks 1 μ apart.

Spectra were obtained with a quadrupole ion trap mass spectrometer (LCQ, Finnigan MAT, San Jose, CA) using the same infusion solvents used for the ESMS experiments. The LCQ was operated manually in the Tune Plus window with nanospray infusion of samples using a novel electrospray interface design (26). The heated desolvation capillary was held at 200°C, with the electron multiplier set to 1.0 kV. The relative collision energy (RCE) was adjusted to obtain diagnostic fragment ion peaks. The RCE varies on this instrument from 0 to 100% for mass analyzer CID, corresponding to 0 to 5 V peak-to-peak resonance excitation RF voltage.

High-resolution FAB mass spectra were obtained with a 6 keV Xe beam and a DMSO–thioglycerol (1/1) plus 1% trifluoroacetic acid matrix on a JEOL HX-110 sector instrument, at a resolution of ca. 7500, with a 10% valley. Approximately 10–20 nmol of sample was used to obtain individual spectra. Polyethylene glycol with mass distribution peaking at *m/z* 300 (PEG 300) was used as an internal calibration standard.

RESULTS

Histidine and N-Acetylhistidine

The synthetic compounds and natural products investigated in this study were adducts of histidine;

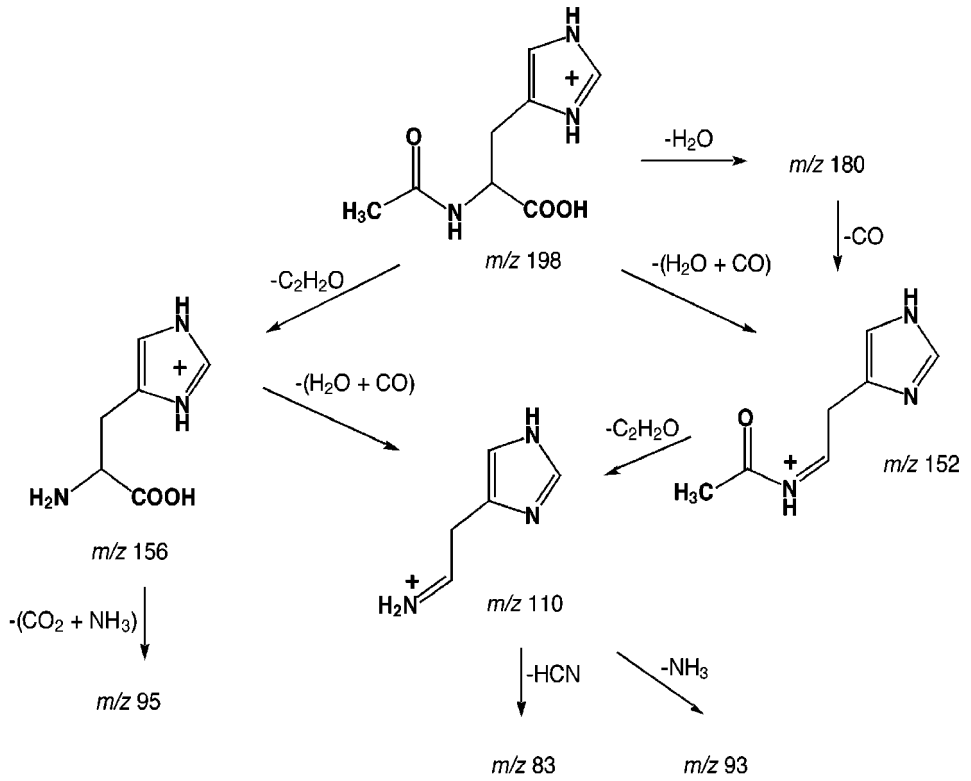

SCHEME 1. Product ions of histidine and *N*-acetylhistidine from ESMS–MS spectra of $[M + H]^+$ precursors.

therefore, the ESMS and ESMS–MS spectra of this amino acid and its *N*-acetyl derivative (NAcHis) were obtained to facilitate interpretation of the fragmentation of the more complex compounds. Product ion formation using $[M + H]^+$ and ions formed by in-source fragmentation as precursors for CID (spectra not shown) were explained primarily by losses of CO_2, H_2O (27) and other side-chain components (Scheme 1, protonation sites based on (28)). In-source fragmentation (fragmentation in the skimmer) refers to formation of product ions at or near the point of introduction of the sample into the mass spectrometer. The standard operating conditions used during these investigations promoted dissociation of the $[M + H]^+$ ions in the skimmer, allowing MS–MS analysis of these product ions formed at the interface of the API III spectrometer.

6-(N-1′)-His-DA

We encountered minor complications in interpreting MS and MS–MS data in the ESMS and ITMS spectra for some of the compounds because the His-DA derivatives had been dissolved previously in deuterated solvents for NMR analysis. Repeated dissolving and evaporation of the two 6-*N*-His-catechol compounds in MeOH or MeOH/H_2O, which should have removed all exchangeable deuteriums, failed to eliminate all of the D, some of which may have been incorporated covalently into the imidazole ring (29, 30). The MS spectra for several of the preparations had peaks corresponding to $[M + H]^+$, $[M + D]^+$, and $[M + 2D\text{-}H]^+$, and the product ion spectra from ESMS–MS of all of these precursors were consistent with the results summarized in the following sections.

For the 6-(*N*-1′)-histidyldopamine (6-(*N*-1′)-His-DA) compound isolated from cuticle hydrolysates (see Fig. 1 for structure), a major product ion of the $[M + H]^+$ precursor at *m/z* 307 was found at *m/z* 261, corresponding to a loss of (CO + H_2O) [Fig. 2]. This was similar to the fragmentation pattern for the (N-1′) isomer of methylhistidine (20). The loss of CO_2 (*m/z* 263) from this precursor was approximately 12% of the intensity of the $(MH - CH_2O_2)^+$ peak (Fig. 2). These conclusions were confirmed by the ESMS–MS and ITMS–MS spectra of *m/z* 308 (not shown), a monodeuterated analog, in which *m/z* 262 was the major product ion. A series of CID spectra obtained using the ion trap and ESMS–MS spectra acquired using precursors formed in the source of the API III mass spectrometer produced fragmentation patterns dominated by loss of CO, H_2O, NH_3, and combinations of these (Figs. 2, 3, and other spectra not shown). Formation of radical cationic product ions, e.g., the quinone methide ion at *m/z* 122, a common phenomenon encountered during electron impact MS of

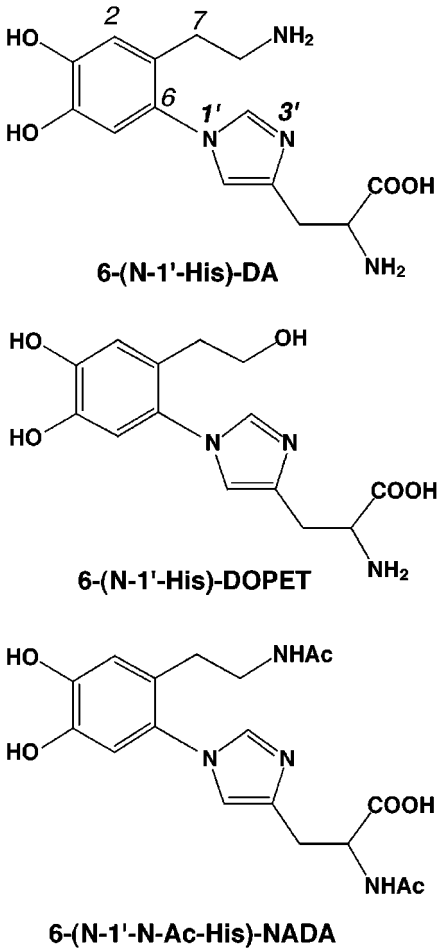

FIG. 1. Structures of histidine-DA, histidine–DOPET, and *N*-acetylhistidine–NADA.

many compounds (19) but rarely documented for ESMS, was invoked to best explain the observed product ions (Fig. 3).

The ITMS–MS spectrum of *m/z* 308 of the (N-1′) isomer showed the expected mass shifts for a compound that had retained deuterium in the imidazole ring (spectrum not shown). Some migration of deuterium into the dopamine ring also occurred. The product ion corresponding to the dopamine ring moiety was present, as were the D^0 (*m/z* 152) and D^1 (*m/z* 153) isotopomers in a 2:1 ratio. In contrast, the intensity of the deuterated ion for the histidyl moiety was twice that of the intensity of the nondeuterated ion.

6-(N-1′)-His–DOPET and Unfractionated M. sexta Cuticle Hydrolysate

The ESMS and ITMS spectra of a compound previously characterized as 6-(*N*-3′)-His-DA (22) consistently produced a prominent $[M + H]^+$ peak at *m/z* 308 rather than one at the expected *m/z* 307. We suspected that this compound might be a His–DOPET rather than a His-DA adduct. High-resolution FAB MS gave an exact mass measurement of 308.1244 m.u., which was in excellent agreement with the theoretical mass for the His–DOPET adduct ($C_{14}H_{18}N_3O_5$) of 308.1245 m.u. The ESMS–MS spectrum (not shown) of the *m/z* 308 precursor had a prominent product ion at *m/z* 262 (loss of H_2O + CO). This was identical to the ESMS–MS spectrum of $[M + H]^+$ of synthetic 6-*N*-His–DOPET, which produced predominantly the *m/z* 262 ion. *N*-His–DOPET ions probably fragment in a manner similar to the corresponding DA adducts, so the synthetic DOPET compound and the adduct isolated from *M. sexta* cuticle were (N-1′) isomers (Scheme 2).

One of the advantages of ESMS and ITMS is the ability to generate significant structural information from unfractionated or partly purified biological samples. To attempt this for histidine–catechol adducts from insect cuticle, an acid hydrolysate from *M. sexta* cuticle was filtered, dried, resuspended in $MeOH/H_2O$, and infused into the spectrometer without any intervening chromatographic steps. ESMS revealed several hundred peaks between *m/z* 75 and 1200. The ion at *m/z* 308 was chosen for further analysis. Based on previous work (22) and results presented here, at least two compounds were expected to contribute to this CID spectrum, 6-*N*-His–DOPET and 7-*N*-His–DOPET (Fig. 4). In addition to peaks observed in the ESMS–MS spectrum of *m/z* 308 from 6-*N*-1′-His–DOPET (*m/z* 262, 247, 235, 230 and 215), the spectrum from the crude hydrolysate had intense product ions in the range from *m/z* 70 to 160 (Fig. 4), which were identical to those generated from ESMS–MS of $[M + H]^+$ of both histidine and *N*-acetylhistidine and also characteristic of 7-linked adducts as discussed in the next section.

7-N-His-DA and 7-N-His–DOPET

Unlike the other compounds investigated, these two adducts had histidyl residues attached to the side chain (C-7) rather than the aromatic ring of the catechol moiety. CID of these compounds produced no diagnostic product ions other than those previously identified for histidine and *N*-AcHis (Scheme 1) at *m/z* 156, 110, 95, 93, and 83 (Fig. 5, *m/z* 307 precursor, spectrum identical for 7-*N*-His–DOPET except for the precursor ion). This would be expected since a benzylic histidyl–catechol bond would be much less stable than an N bond to an aromatic ring. The compound tentatively identified as 7-(*N*-3′)-His-DA (22) had an $[M + H]^+$ ion at *m/z* 308, consistent with it being a DOPET instead of a DA adduct. Lack of product ions in the higher mass range of spectra, obtained even when a wide range of CID gas densities and potential differences between the source and detector was used, precluded assignment of an (N-1′) or (N-3′) attachment site for the catechol to the imidazole ring.

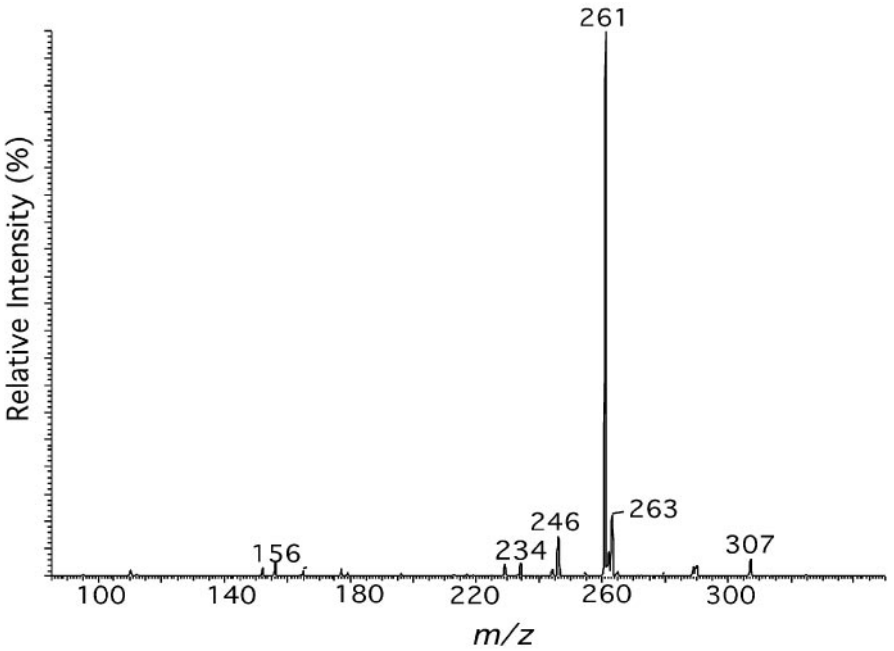

FIG. 2. ITMS–MS spectrum of 6-(*N*-1′)-His-DA: $[M + H]^+$ (*m*/z 307) precursor.

2-(N-3′)-NAcH–NADA

Spectra of 2-(*N*-3′)-NAcH–NADA were consistent with the structure obtained using other spectroscopic techniques (21). The CID spectra indicated that this compound was the (N-3′) isomer, with prominent product ion peaks at *m/z* 347 (loss of CO_2) for the *m/z* 391 precursor (Fig. 6, Scheme 2) and at *m/z* 348 for the (monodeuterated) *m/z* 392 precursor (spectrum not shown). Product ions corresponding to loss of (H_2O + CO) from $[M + H]^+$ (*m/z* 346 and 345 for precursors at 392 and 391) were present, but these were ca. 6× less intense than the product ions formed from loss of CO_2. In addition to the many product ions in common with those from 6-(*N*-1′)-NAcH–NADA, the ESMS–MS and ITMS spectra (not shown) of 2-(*N*-3′)-NAcH–NADA had a product ion of moderate intensity at *m/z* 305 from loss of (C_2H_2O + CO_2), providing further support that this compound was the (N-3′) isomer of 2-NAcH–NADA.

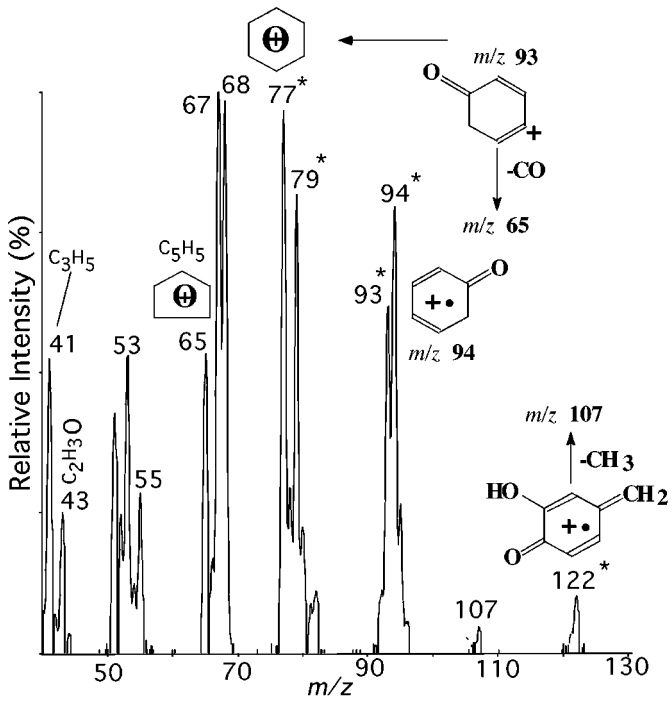

FIG. 3. ESMS–MS spectrum of *m/z* 122 product ion from 6-(*N*-1′)-His-DA. Product ions marked by an * also were selected as precursors for CID analysis.

6-(N-1′)-NAcH–NADA

The final model compound analyzed was 6-NAcH–NADA. A prominent product ion at *m/z* 345 [loss of (H_2O + CO)] from CID of the *m/z* 391 precursor in ESMS–MS and ITMS–MS spectra suggested that this compound was the (N-1′) isomer (spectra not shown). Product ions at *m/z* 349 and 303 were due to the loss of C_2H_2O from one of the two N-linked acetyl groups and loss of [C_2H_2O + (H_2O + CO)], respectively. Formation of less-intense product ions at *m/z* 373 (loss of H_2O), *m/z* 327 (*m/z* 345 − H_2O), *m/z* 288 (loss of CO_2 + $AcNH_2$), and *m/z* 229 (*m/z* 288 − $AcNH_2$) was confirmed by ESMS–MS of precursors formed in the source.

The ITMS–MS spectra, in addition to product ions observed in ESMS–MS experiments, had product ions corresponding to: 391 − CO_2 (minor peak, *m/z* 347),

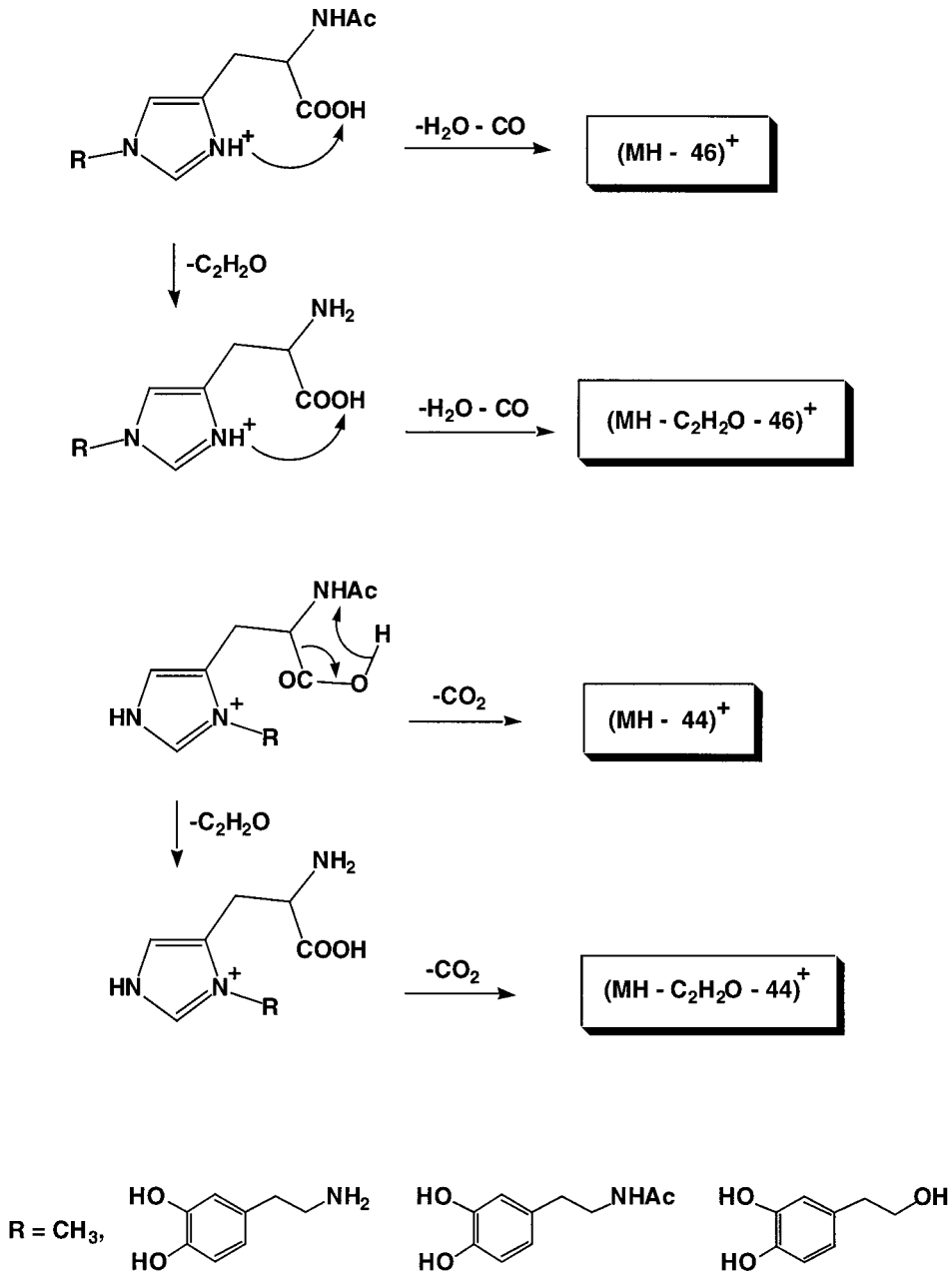

SCHEME 2. Diagnostic product ions for histidine-(*N*-1′)– and histidine-(*N*-3′)–catechol adducts.

391 − $AcNH_2$ (*m/z* 332), 391 − [C_2H_2O + H_2O] (*m/z* 331), *m/z* 347 − H_2O (*m/z* 329), *m/z* 345 − H_2O (*m/z* 327), 391 − [H_2O + $AcNH_2$] (*m/z* 314), and *m/z* 345 − $AcNH_2$ (*m/z* 286). The ITMS–MS spectra of the monodeuterated analog *m/z* 392 precursor were consistent with these fragmentations (spectra not shown).

DISCUSSION

Catechols, catecholamines, and their quinone derivatives and peptide adducts have significant biological activities and structural functions (31–36). Recent reports of the involvement of quinone methides in carcinogenesis (37–40) and their widespread relevance in organic and biological chemistry (34, 41) have spurred further development of techniques to characterize compounds formed via these reactive intermediates. In insects, in addition to their role in cuticular sclerotization (10–12), quinone-mediated polymerization of polyphenols and related tanning reactions have been implicated in cuticular defense against microbial invasion (42, 43), and in determination of susceptibility to infection of mosquitoes and other insects by filarial worms,

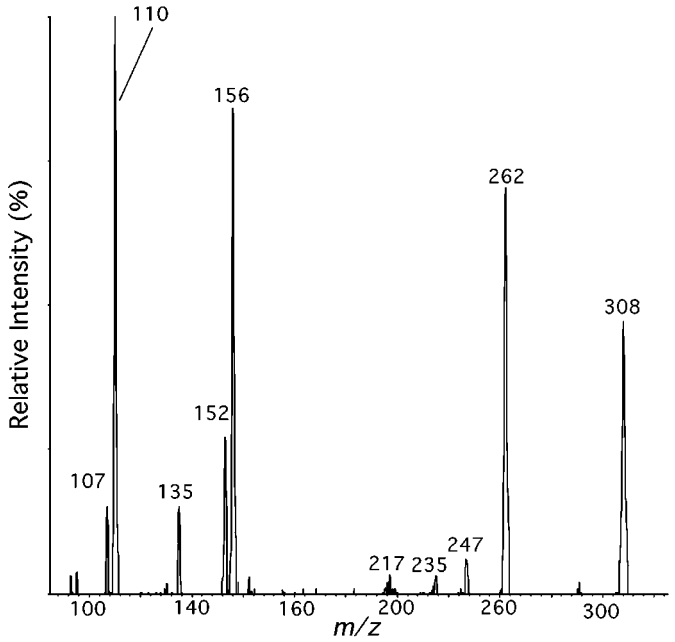

FIG. 4. ESMS–MS spectrum of 6-(*N*-1′)-His–DOPET: $[M + H]^+$ (*m*/z 308) precursor.

plasmodia responsible for malaria, and other parasites (44, 45).

Solid-state ^{13}C and ^{15}N NMR have been used to characterize aromatic cross-links as well as for compositional analyses of insect and other invertebrate sclerotized structures (16, 32, 46–48). The noninvasive nature of this technique provides information on unmodified, intact cuticle but cannot provide detailed structural data and requires rather large amounts of sample. Other approaches have used HPLC with either electrochemical or diode array detection in the UV region, in combination with NMR and mass spectrometry (primarily FAB), to characterize condensation products of oxidized catechols and catecholamines with other phenolic compounds, amino acids, and peptides (13–18, 21, 22).

Classical chemical techniques used in earlier studies were summarized in a comprehensive review (49). Pyrolysis/gas chromatography/mass spectrometry also has proven useful in analysis of invertebrate cuticle (50, 51). FAB MS has been used for structural analyses of these compounds, but background signals from the matrix into which samples must be incorporated limit sensitivity, especially in the lower mass range. To provide unambiguous structural information, compounds

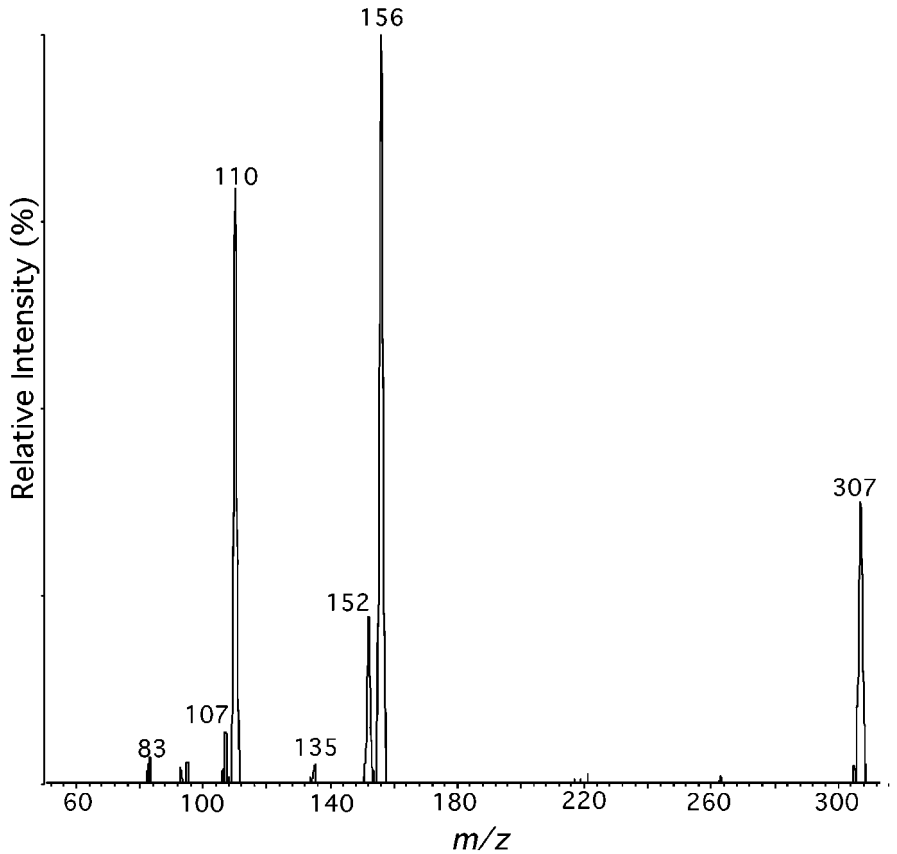

FIG. 5. ESMS–MS spectrum of *Manduca sexta* cuticle hydrolysate: $[M + H]^+$ (*m*/z 307) precursor.

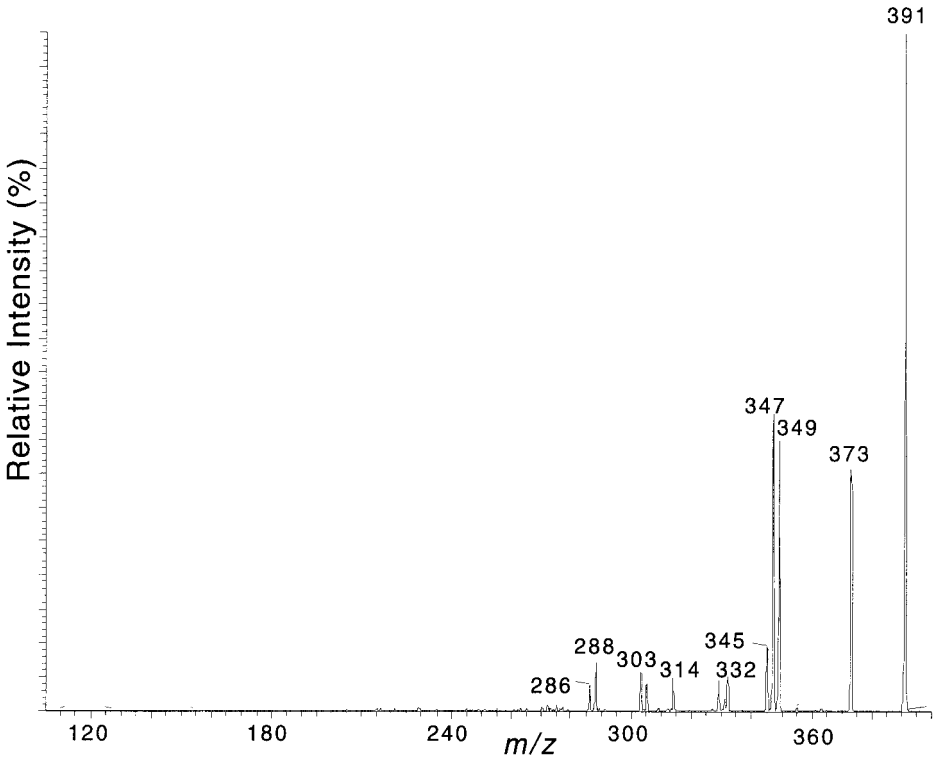

FIG. 6. ITMS–MS spectrum of 2-(*N*-3′)-NAcH–NADA: $[M + H]^+$ (*m*/z 391) precursor.

must be relatively pure for FAB MS. MALDI–TOF MS has less of a problem with matrix peaks, although the lower mass range is again problematic. MALDI is generally more sensitive than FAB, with 10–1000 pM concentrations sufficient to generate useful spectra for most compounds; however, like FAB, the capability of MALDI to generate useful structural information from multicomponent mixtures is limited.

Recently, MALDI–TOF MS (52) and ESMS–MS (53) have been used to characterize polyphenols, catecholamines, and their oxidation products. ESMS also has been used to profile protein and peptide adducts of oxidized phenols (54, 55). These initial efforts and this report have demonstrated the utility of ESMS(–MS) and ITMS(–MS) in studies on catechols and the products resulting from the reactions of quinones and other oxidation products. Complex mixtures from hydrolysates of insect cuticle and other natural products can be analyzed using these two MS techniques, with minimal preliminary chromatography, by exploiting the MS–MS capabilities of triple quadrupole electrospray instruments and MS^n experiments using ion trap spectrometers.

Characterization of cross-linking between cuticular catecholamines with peptides and proteins has been the focus of much research using both hydrolysates of insect cuticle and *in vitro* incubation of model substrates with cuticular enzymes (12, 13, 15, 16, 46, 56–58). Previously, we assumed that all adducts were in the His-DA class, because the NMR methods utilized could not unequivocally differentiate between His-DA and His–DOPET structures. The His–DOPET type of adducts characterized in this study is a new discovery.

ITMS and ESMS can be used to identify the site on the imidazole ring to which catecholamines are attached to the aromatic ring (20), providing a facile and definitive method for defining subtle structural features of this class of compounds. These types of MS analyses will be extended next to study more complex peptide–polyphenol polymers and catecholamine–amine conjugates involving chitin and/or chitosan, as well as to characterize the compositions of exoskeletons from a number of other insect species.

ACKNOWLEDGMENTS

This work was supported in part by grants from the National Institutes of Health (AI 34339) to J.L.K. and the National Science Foundation (MCB-9418129) to T.L.H. and K.J.K. Cooperative investigation between the University of Washington, the U.S. Department of Agriculture, and the Kansas Agricultural Experiment Station (Contribution No. 98-467-J). Mention of a proprietary product does not constitute a recommendation by the USDA. The Agricultural Research Service, USDA, is an equal opportunity/affirmative action employer, and all agency services are available without discrimination.

REFERENCES

1. Parekh, R. B., and Rohlff, C. (1997) *Curr. Opin. Biotechnol.* **8,** 718–723.

2. Kuster, B., and Mann, M. (1998) *Curr. Opin. Struct. Biol.* **8,** 393–400.
3. Yan, J. X., Packer, N. H., Gooley, A. A., and Williams, K. L. (1998) *J. Chromatogr.* **808A,** 23–41.
4. Zhang, X. L., Herring, C. J., Romano, P. R., Szczepanowska, J., Brezska, H., Hinnebusch, A. G., and Qin, J. (1998) *Anal. Chem.* **70,** 2050–2059.
5. Reising, K. A., and Ahn, N. G. (1997) *Cell Cycle Control* **283,** 29–44.
6. Quest, A. F. G., Harvey, D. J., and McIlhinney, R. A. J. (1997) *Biochemistry* **36,** 6993–7002.
7. Dietrich, A., Brazil, D., Jensen, O. N., Meister, M., Schrader, M., Moomaw, J. F., Mann, M., Illenberger, D., and Gierschik, P. (1996) *Biochemistry* **35,** 15174–15182.
8. James, D. C. (1996) *Cytotechnology* **22,** 117–124.
9. Haltiwanger, R. S., Grove, K., and Philipsberg, G. A. (1998) *J. Biol. Chem.* **273,** 3611–3617.
10. Andersen, S. O. (1990) *in* Molting and Metamorphosis (Ohnishi, E., and Ishizaki, H., Eds.), pp. 133–155, Springer-Verlag, Berlin.
11. Hopkins, T. L., and Kramer, K. J. (1992) *Annu. Rev. Entomol.* **37,** 273–302.
12. Andersen, S. O., Peter, M. G., and Roepstorff, P. (1996) *Comp. Biochem. Physiol. B* **113,** 689–705
13. Andersen, S. O., Jacobsen, J. P., and Roepstorff, P. (1992) *Insect Biochem. Molec. Biol.* **22,** 517–527.
14. Andersen, S. E., Jacobsen, J. P., Roepstorff, P., and Peter, M. G. (1991) *Tetrahedron Lett.* **34,** 4287–4290.
15. Sugumaran, M., Ricketts, D. (1995) *Arch. Insect Biochem. Physiol.* **28,** 17–32.
16. Christensen, A. M., Schaefer, J., Kramer, K. J., Morgan, T. D., and Hopkins, T. L. (1991) *J. Am. Chem. Soc.* **113,** 6799–6802.
17. Kramer, K. J., Morgan, T. D., Hopkins, T. L., Christensen, A. M., and Schaefer, J. (1989) *Insect Biochem.* **19,** 753–757.
18. Kramer, K. J., Hopkins, T. L., and Schaefer, J. (1995) *Insect Biochem. Molec. Biol.* **25,** 1067–1080.
19. Schaefer, J., Kramer, K. J., Garrow, J. R., Jacob, G. S., Stejskal, E. O., Hopkins, T. L., and Speirs, R. D. (1987) *Science* **235,** 1200–1204.
20. Turecek, F., Kerwin, J. L., Xu, R., and Kramer, K. J. (1998) *J. Mass Spectrom.* **33,** 392–396.
21. Xu, R., Huang, X., Morgan, T. D., Prakash, O., Kramer, K. J., and Hawley, M. D. (1996) *Arch. Biochem. Biophys.* **329,** 56–64.
22. Xu, R. D., Huang, X., Hopkins, T. L., and Kramer, K. J. (1997) *Insect Biochem. Mol. Biol.* **27,** 101–108.
23. Hopkins, T. L., Morgan, T. D., and Kramer, K. J. (1984) *Insect Biochem.* **14,** 533–540.
24. Huang, X., Xu, R., Hawley, M. D., and Kramer, K. J. (1997) *Bioorg. Chem.* **25,** 179–202.
25. Wang, H., Lim, K. B., Lawrence, R. F., Howald, W. N., Taylor, J. A., Ericsson, L. H., Walsh, K. A., and Hackett, M. (1997) *Anal. Biochem.* **250,** 162–168.
26. Gatlin, C. L., Kleeman, G. R., Hays, L. G., Link, A. J., and Yates, J. R., III (1998) *Anal. Biochem.* **263,** 93–101.
27. McLafferty, F. W., and Turecek, F. (1993) Interpretation of Mass Spectra, 4th ed. University of Science Books, Sausalito, CA.
28. Nguyen, V. Q., and Turecek, F. (1996) *J. Mass Spectrom.* **31,** 1173–1184.
29. Gillespie, R. J., Grimison, A., Ridd, J. H., and White, R. F. (1958) *J. Chem. Soc.* 3228–3229.
30. Vaughan, J. D., Mughrabi, Z., and Wu, E. C. (1970) *J. Org. Chem.* **35,** 1141–1145.
31. Niznik, H. B. (Ed.) (1994) Dopamine Receptors and Transporters: Pharmacology, Structure, and Function, pp. 1–677, Dekker, New York.
32. Ali, D. W. (1997) *J. Exp. Biol.* **200,** 1941–1949.
33. Manger, P., Li, J., Christensen, B. M., and Yoshino, T. P. (1996) *Comp. Biochem. Physiol. A* **114,** 227–234.
34. Peter, M. G. (1989) *Angew. Chem. Int. Ed. Engl.* **28,** 555–570.
35. Sugumaran, M. (1991) *FEBS Lett.* **293,** 4–10.
36. Prota, G. (1992) Melanins and Melanogenesis, pp. 1–87, Academic Press, San Diego.
37. Bolton, J. L., and Shen, L. (1996) *Carcinogenesis* **17,** 925–929.
38. Thompson, D. C., Perera, K., Krol, E. S., and Bolton, J. L. (1995) *Chem. Res. Toxicol.* **8,** 323–327.
39. Mayalarp, S. P., Hargreaves, R. H. J., Butler, J., O'Hare, C. C., and Hartley, J. A. (1996) *J. Med. Chem.* **39,** 531–537.
40. Wan, P., Barker, B., Diao, L, Fischer, M., Shi, Y., and Yang, C. (1996) *Can. J. Chem.* **74,** 465–4475.
41. Sugumaran, M., Semensi, V., Kalyanaraman, B., Bruce, J. M., and Land, E. J. (1992) *J. Biol. Chem.* **267,** 10355–10361.
42. Shida, M, and Brey, P. T. (1995) *Proc. Natl. Acad. Sci. USA* **92,** 10698–10702.
43. Christensen, B. M., and Tracy, J. W. (1989) *Am. Zool.* **29,** 387–398.
44. Nayar, J. K., and Knight, J. W. (1995) *J. Invertebr. Pathol.* **65,** 295–299.
45. Lee, W.-J., Ahmed, A., della Torre, A., Kobayashi, A., Ashida, M., and Brey, P. T. (1998) *Insect Mol. Biol.* **7,** 41–50.
46. Kramer, K. J., Hopkins, T. L., and Schaefer, J. (1995) *Insect Biochem. Mol. Biol.* **25,** 1067–1080.
47. Holl, S. M., Schaefer, J., Goldberg, W. M., Kramer, K. J., Morgan, T. D., and Hopkins, T. L. (1992) *Arch. Biochem. Biophys.* **292,** 107–111.
48. Andersen, S. O., Jacobsen, J. P., Bojesen, G., and Roepstorff, P. (1992) *Biochim. Biophys. Acta* **1118,** 134–138.
49. Brunet, P. C. J. (1980) *Insect Biochem.* **10,** 467–500. 50 . Stankiewicz, B. A., van Bergen, P. F., Duncan, I. J., Carter, J. F., Briggs, D. E. G., and Evershed, R. P. (1996) *Rapid Commun. Mass Spectrom.* **10,** 1747–1757.
51. Stankiewicz, B. A., Mastalerz, M., Hof, C. H. J., Bierstedt, A., Flannery, M. B., Briggs, D. E. G., and Evershed, R. P. (1998) *Org. Geochem.* **28,** 67–76.
52. Kroesche, C., and Peter, M. G. (1996) *Tetrahedron* **52,** 3947–3952.
53. Kerwin, J. L. (1996) *J. Mass Spectrom.* **31,** 1429–1439.
54. Bolton, J. L., Le Blanc, J. Y. C., and Siu, K. W. M. (1993) *Biol. Mass Spectrom.* **22,** 666–668.
55. Kerwin, J. L. (1997) *Rapid Commun. Mass Spectrom.* **11,** 557–566.
56. Sugumaran, M., Dali, H., and Semensi, V. (1989) *Arch. Insect Biochem. Physiol.* **11,** 127–137.
57. Andersen, S. O., Peter, M. G., and Roepstorff, P. (1992) *Insect Biochem. Mol. Biol.* **22,** 459–469.
58. Okot-Kotber, B. M., Morgan, T. D., Hopkins, T. L., and Kramer, K. J. (1996) *Insect Biochem. Mol. Biol.* **26,** 475–484.